# High Power Dynamic Polarization Control Using Plasma Photonics

D. Turnbull,[1,*] P. Michel,[1] T. Chapman,[1] E. Tubman,[2] B. B. Pollock,[1] C. Y. Chen,[3] C. Goyon,[1] J. S. Ross,[1] L. Divol,[1] N. Woolsey,[2] and J. D. Moody[1]

[1]*National Ignition Facility, Lawrence Livermore National Laboratory, Livermore, California 94550, USA*
[2]*York Plasma Institute, University of York, Heslington, York YO10 5DQ, United Kingdom*
[3]*School of Electrical and Computer Engineering, Cornell University, Ithaca, New York 14853, USA*

(Received 8 March 2016; published 18 May 2016)

We report the first experimental demonstration of a plasma wave plate based on laser-induced birefringence. An elliptically polarized input was converted into a nearly ideal circularly polarized beam using an optical system composed of a second laser beam and a plasma. The results are in excellent agreement with linear theory and three-dimensional simulations up to phase delays exceeding $\pi/4$, thus establishing the feasibility of laser-plasma photonic devices that are ultrafast, damage-resistant, and easily tunable.

DOI: 10.1103/PhysRevLett.116.205001

The interactions between intense laser beams and plasmas have broad and far-reaching applications in applied and fundamental science, such as inertial confinement fusion (ICF) [1], laboratory astrophysics [2], and particle acceleration [3,4], to name a few. Plasmas can also be used to manipulate the basic properties of light waves, which could revolutionize the design and applications of high-power lasers; the use of plasma in lieu of conventional optics alleviates the constraints associated with optic damage, which is currently one of the main factors driving the size and cost of large-scale laser facilities. Examples of plasma-based optical components include plasma mirrors [5], which can be used to redirect, focus, and improve the contrast of laser beams, plasma gratings, which are routinely used at the National Ignition Facility to tune the implosion symmetry of ICF targets by facilitating power transfer between intense lasers [6–8], laser amplifiers [9,10], and laser compressors [11]. More recently, we showed theoretically that plasmas could also be used to dynamically control the polarization of light waves [12]. In this Letter, we present the first experimental demonstration of a high power, tunable, ultrafast plasma wave plate. Birefringence was induced in the plasma via an auxiliary "pump" laser beam; the phase retardation of the [pump + plasma] optical system was remotely controlled by varying the plasma density and pump intensity. The polarization of a "probe" beam propagating through that optical system was converted from elliptical to circular by appropriately tuning these parameters. Plasma-mediated polarization control enables more sophisticated manipulation of light at fluences millions of times greater than those withstood by traditional (crystal-based) optics.

The optical properties of a plasma as seen by a probe laser beam with electric field $E_1$ and frequency $\omega_1$ can be modified by adding an auxiliary ("pump") laser beam with $E_0$ and $\omega_0$. The presence of the pump introduces optical resonances when the probe frequency $\omega_1 = \omega_0 \pm \omega_p$, where $\omega_p$ is the frequency of a plasma mode (either an electron-plasma wave or an ion acoustic wave) with wave number $k_b = |\boldsymbol{k}_0 - \boldsymbol{k}_1|$. At resonance, the amplitude of the probe beam undergoes exponential growth or decay due to energy transfer from or to the pump beam via a three-wave coupling process. In turn, as described by the Kramers-Kronig relations, the frequency-dependent variation of the probe's amplitude in the vicinity of an optical resonance must be accompanied by a variation in the refractive index seen by the probe. In the particular situation where $\omega_0 = \omega_1$, the probe's frequency sits in between the two anti-symmetric Stokes and anti-Stokes ion-acoustic resonances at $\omega_0 \pm \omega_{\mathrm{IAW}}$. Assuming the laser frequency bandwidths are small relative to the ion acoustic frequency, the probe's amplitude remains unchanged (no energy exchange with the pump), but it experiences a net refractive index increase from $\eta_0 = (1 - n_e/n_c)^{1/2}$, the background plasma refractive index where $n_e$ is the electron density and $n_c$ is the critical density for the probe's frequency $\omega_1$, to $\eta_0 + \delta\eta$ [cf. Fig. 1(a)]. Using a Jones analysis, we recently showed, theoretically, [12] that the refractive index modification was only experienced by the "$\mathbf{E}_{1\parallel}$" component of the probe's electric field parallel to the projection of $\mathbf{E}_0$ in the probe's plane of polarization [cf. Fig. 1(b), where $\mathbf{E}_0$ is shown in the plane of the pump and probe $\boldsymbol{k}$ vectors as was the case in the experiments described below]. The orthogonal "$\mathbf{E}_{1\perp}$" component, on the other hand, remains unaffected and only sees the background refractive index $\eta_0$. The [pump + plasma] optical system seen by the probe is thus birefringent. The full expression for the refractive index perturbation $\delta\eta$ was derived in Michel *et al.* [12] using a kinetic plasma model; using a fluid approximation for the plasma, the phase retardation $\Delta\phi = \delta\eta k_1 L$ between the probe's electric field components along the slow and fast axes is given by the simple formula

 

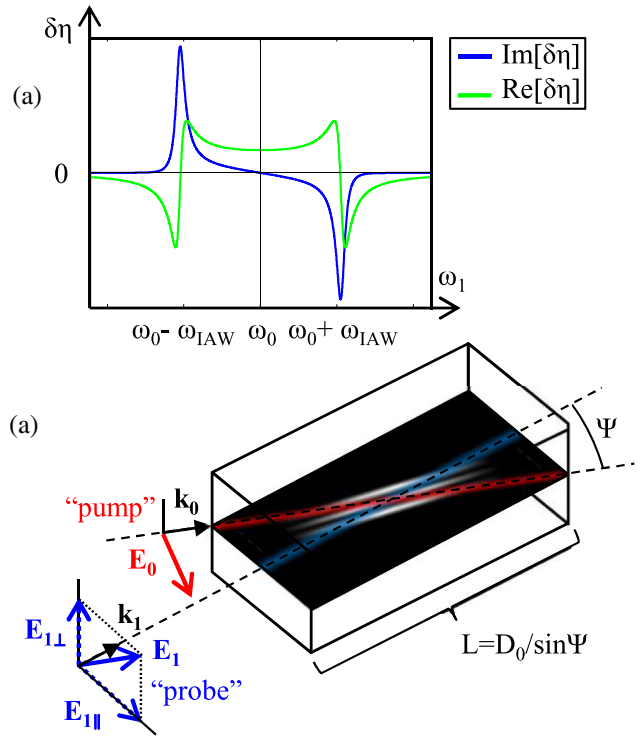


FIG. 1. Part (a) shows the real and imaginary components of the refractive index modulation induced by the [pump + plasma] system. When $\omega_1 = \omega_0$, the imaginary component disappears (absence of energy transfer) but the real component is nonzero (induced birefringence). Part (b) illustrates the probe interacting with the plasma wave plate. An ideal quarter or half wave plate requires the probe polarization to have equal components parallel and perpendicular to the pump polarization.

$$\Delta\phi = 1.68 \times 10^{-11} \lambda_0[\mu\text{m}] L[\text{mm}] \frac{n_e/n_c}{T_e[\text{keV}]} [I_p \cos(\psi) + I_s], \tag{1}$$

where $\lambda_0$ is the laser wavelength, $L$ is the propagation length of the probe through the optical system, $T_e$ is the electron temperature, and $I_p$ ($I_s$) denotes the pump intensity projected in the plane of (orthogonal to) the pump and probe intersection (in [W/cm$^2$]).

Here we present the first experimental demonstration of a laser-plasma wave plate, operating exclusively on the beam's phase rather than amplitude, which was conducted at Lawrence Livermore National Laboratory's Jupiter Laser Facility on the Janus laser. A variable back pressure gas jet, fitted with a 3 mm-outlet-diameter supersonic nozzle, released helium gas prior to the arrival of the laser beams. A high energy pump and low energy probe (both with $\lambda = 1.053$ $\mu$m) were overlapped over the gas jet with a crossing angle of 27°. A continuous phase plate in the pump beam path gave it a 600 $\mu$m diameter at best focus, and the probe was tightly focused over the nozzle and nearly diffraction limited for an $f/6.7$ beam. The pump was horizontally polarized, and the probe was initially elliptically polarized; the orientation angle of the ellipse was close to 45° such that $|\mathbf{E}_{1\parallel}| \approx |\mathbf{E}_{1\perp}|$, and $\mathbf{E}_{1\parallel}$ was delayed 38° with respect to $\mathbf{E}_{1\perp}$. We used ≈3 ns square and ≈250 ps Gaussian pulse shapes for the pump and probe, respectively. The high energy pump ionized the gas and set the plasma conditions prior to the arrival of the probe, which was timed to overlap with the latter half of the pump beam. Thomson scattered light from the pump pulse was collected at a scattering angle of 90° and directed to a streaked spectrometer that measured the blue-shifted electron-plasma wave feature, which was used to determine the electron density and temperature at the center of the interaction region. An 800 nm-wavelength nonperturbing diagnostic beam was also incident on the plasma orthogonal to the pump and co-timed with the probe; this beam was sent to a Mach-Zehnder interferometer and used to diagnose gradients in the density distribution.

By appropriately tuning the plasma parameters, the laser-plasma induced phase delay was made to complement the incident probe ellipticity in order to give the probe a nearly ideal circular polarization (the delay between the probe's horizontal and vertical components became 90.3°). This is shown in Fig. 2. Both the initial [Fig. 2(a)] and final [Fig. 2(b)] probe polarizations were determined by imaging the interaction plane onto a CCD camera through a Wollaston prism, which was oriented so as to separate the 45° and 135° polarization components. The phase delay between the horizontal and vertical components of the probe polarization can be determined by the relative signal energies, denoted $U_{45°}$ and $U_{135°}$, by the formula

$$\Delta\phi = 2\tan^{-1}(\sqrt{U_{135°}/U_{45°}}). \tag{2}$$

The single measurement, however, is not unambiguous. If an alternate process made the probe polarization horizontal, vertical, or unpolarized, the same result would be obtained ($U_{45°} = U_{135°}$). To break this degeneracy, the shot shown in Fig. 2(b) was repeated (replicating all parameters to within 5%) with the addition of a quartz $\lambda/4$ wave plate before the Wollaston prism. With the fast axis oriented vertically, the circular polarization was restored to linear and the orthogonal component was almost completely extinguished as shown in Fig. 2(c). This verified that the laser-plasma wave plate had in fact made the polarization circular to high accuracy.

During the experiment, the observed phase delay was inferred from the probe polarimetry diagnostic using Eq. (2). Figure 3 shows each data point compared with the expected phase delay calculated from Eq. (1). Density, temperature, and intensity were all measured, and the interaction length was determined by the pump diameter (set by the 600 $\mu$m phase plate) and the pump-probe crossing angle. Density and pump intensity were the primary parameters that were adjusted to tune the phase

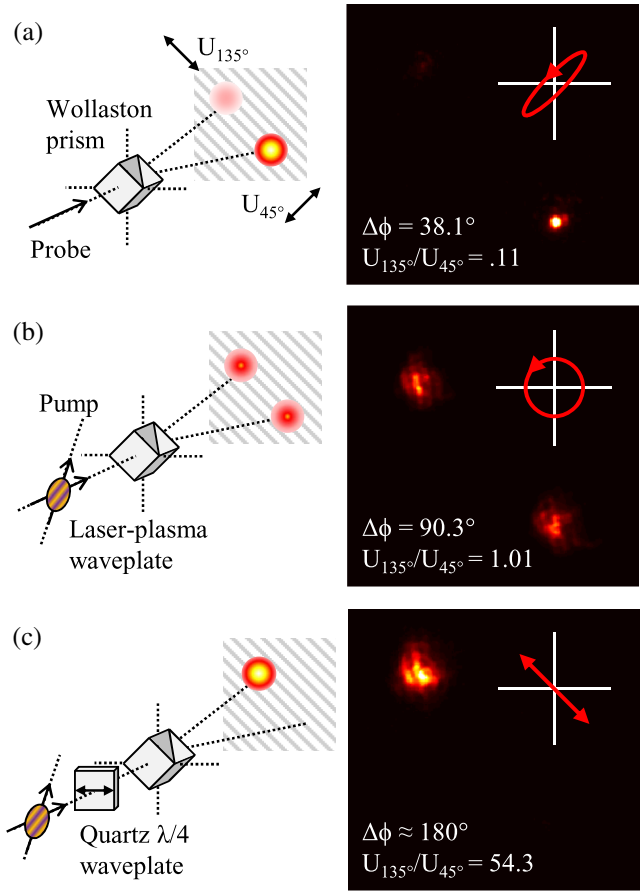


FIG. 2. Part (a) shows that the probe is initially elliptical with an orientation close to 45° and a phase delay of 38° between its horizontal and vertical components. (b) With optimized conditions, the laser-plasma wave plate induced an additional ≈52° delay such that the probe became nearly ideally circularly polarized. (c) This was verified on a subsequent shot by inserting a crystal quarter wave plate into the probe beam path to convert from circular back to linear polarization.

delay. The pump energy was varied from 150–700 J, yielding intensities between $I \approx (2\text{–}10) \times 10^{13}$ W cm$^{-2}$. For comparison, the probe energy was ≈100 mJ and focused to an intensity ≈$10^{11}$ W/cm$^2$ in the plasma. Note that no effort was made to optimize the efficiency of the device by minimizing the necessary pump laser energy. The laser energy budget allowed us to use a large pump spot size and relatively long duration laser pulse, which minimized uncertainties associated with laser pointing and timing jitter, but the fraction of the pump actually overlapping the probe in time and space was on the order of a few percent. Each data set in the plot corresponds to a different gas jet back pressure, which was used to control the plasma density. The actual density spanned $n_e = (0.65\text{–}3.35) \times 10^{19}$ cm$^{-3}$ for these parameters. Higher densities allowed access to larger phase delays in accordance with the theory, and, in general, the agreement is excellent when the product of pump intensity and electron

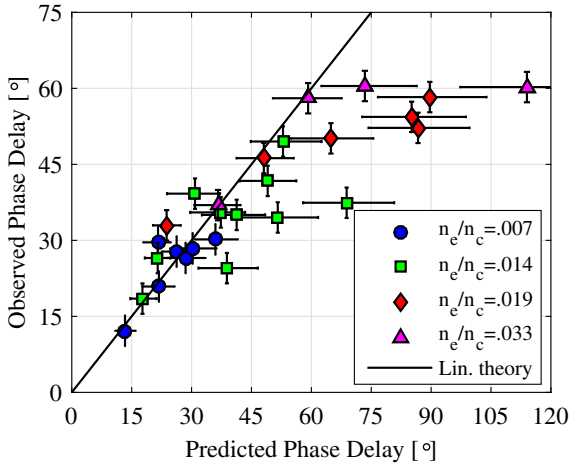


FIG. 3. The measured phase delays are compared against the predicted phase delays from linear theory. The data agree quite well with the linear theory at low density and intensity but diverge at predicted phase delays $\Delta\phi \gtrsim 50°$. Simulations performed with PF3D indicate that this nonlinearity is due to transient effects when the system is strongly driven.

density is low (the linear best fit for $n_e/n_c = .007$ is $y/x = .97$ with $R^2 = .58$ whereas perfect agreement would be $y/x = 1$). However, the predicted phase delays do not scale linearly with pump energy and electron density because both also increase the electron temperature via inverse bremsstrahlung absorption. $T_e$ was measured to be $180 \pm 20$ eV at the lowest density and pump energy and $380 \pm 40$ eV at the highest density and pump energy. At the higher densities and intensities, the experimental results appear to diverge from the linear theory despite accounting for the moderating effect of the increased temperature.

We believe that the deviation from linearity is due to transient effects. While the steady-state response of the system in this frequency-degenerate case involves a phase delay without any energy transfer, the beat wave initially drives a transient grating [13] that can transfer energy, which would violate an assumption built into the polarimetry data analysis. The system should reach steady state in a time $\tau_{\text{sat}} \approx \Delta\phi/(2\nu^2\omega_{\text{IAW}})$, where $\nu$ is the ion acoustic damping rate (normalized to the ion acoustic frequency); this becomes comparable to the probe pulse duration as the pump intensity is increased in these weakly damped plasmas.

To gain additional insight, three-dimensional simulations modeling the propagation of both beams through the plasma were performed with the code PF3D [14]. Plasma and laser parameters were specified based on the experimental conditions. Cross sections of the simulation setup are shown in Figs. 4(a) and 4(b). Simulation results were in good agreement with the data and the linear theory given by Eq. (1) for predicted phase delays up to $\Delta\phi \approx 50°$. Figure 4 shows a simulation in this regime. In Fig. 4(c), the driven IAW (short-scale structure) is apparent, as well as

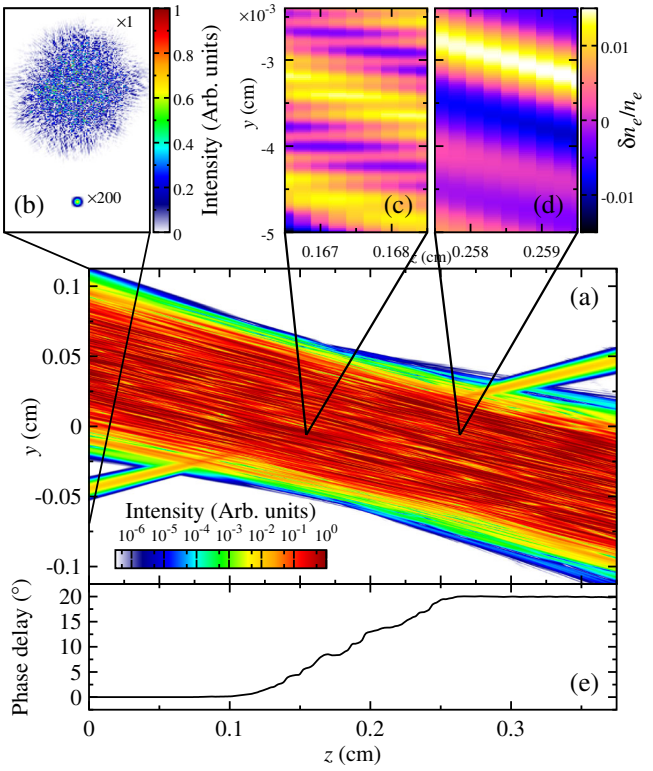


FIG. 4. PF3D simulations of the experiment. (a) The simulation domain is 3.75 mm long, fully containing the 600 $\mu$m diameter pump (with a speckle pattern characteristic of phase plates) and 30 $\mu$m diameter probe [both shown in part (b)]), which overlap with a crossing angle of 27°. (c) The electron density modulation driven by the beat wave is superimposed on the bulk hydrodynamic motion driven by the pump's speckle pattern, the latter of which is isolated in part (d) showing a region of plasma where the probe beam is not present. (e) Intense speckles prompt discrete jumps in the probe phase shift, which steadily accumulates as the probe interacts with the pump beam and levels off once the pump and seed have separated spatially within the plasma.

the response of the plasma to the inhomogeneous light pressure of the speckled pump beam (long-scale structure), the latter of which is isolated in Fig. 4(d) showing a region of plasma absent the probe beam. In Fig. 4(e), the phase delay $\Delta\phi$ is plotted as a function of $z$; it accumulates along the region of pump-probe overlap and increases rapidly through intense laser speckles. However, under conditions where the phase delay was expected (based on linear theory) to exceed $\Delta\phi \approx 50°$, simulations did not reach a steady state within the duration of the probe pulse. In these cases, significant pump-probe power transfer occurred, and a direct and unambiguous measurement of the birefringence-induced phase delay could not be made. Our simulation results are therefore consistent with both the linear theory and the hypothesis that transient effects in these weakly damped He plasmas affected the experimental measurement of polarization as pump intensity and plasma density were increased.

This limit can be avoided by increasing the interaction length rather than continuing to increase density and/or intensity. Indeed, a limited number of additional shots were conducted using a different phase plate giving the pump beam a 1 mm diameter, which increases the interaction length $L \approx D/\sin(\psi)$. The larger beam diameter did limit the intensities that it was possible to access, and the density was lower in the additional overlap regions far from the center of the plasma, but nevertheless the larger interaction length enabled the largest absolute phase delay (61.5°) as well as larger phase delays than companion shots with comparable density and intensity but smaller pump diameter. The interaction length can also be extended by reducing the crossing angle between pump and probe. Increasing the ion acoustic damping rate should also limit degradation due to transient effects at high plasma density and pump intensity.

In summary, we have demonstrated for the first time that a wave plate based on laser-induced plasma birefringence can be used to alter a probe laser's polarization. An elliptically polarized input was converted into a nearly ideal circularly polarized beam by inducing a phase delay of ≈52° in plasma, and the maximum phase delay reached 61.5°. A probe's polarization is easily tuned by varying the pump intensity, plasma density, and/or interaction length. The results are in excellent agreement with linear theory up to phase delays exceeding $\Delta\phi = \pi/4$. Deviation from linearity at larger predicted phase delays may be due to transient effects in the weakly damped plasmas that were used in this experiment. Several remediation pathways should allow access to the 180° phase delay needed to have complete control over a laser's state of polarization. This demonstrates the potential for high-power, tunable laser-plasma photonic devices.

There are also numerous implications for existing experiments that employ multiple crossed laser beams. One is that the polarization change induced in a probe beam by a crossing pump can be used to diagnose plasma conditions. Another is that a certain amount of polarization smoothing [15,16], with benefits such as reduced laser-plasma instability growth and less laser self-focusing, is intrinsic to situations in which multiple laser beams cross at arbitary angles in plasma, such as in the laser entrance holes of indirect-drive inertial confinement fusion hohlraums. This may also mean that polarization alteration could impact the modeling of crossed-beam energy transfer [6–8] in both indirect- and direct-drive ICF. Understanding laser-plasma impacts on polarization is critical in situations in which polarization affects both laser absorption and ion acceleration mechanisms [17,18]. Finally, plasma-mediated polarization control complements the suite of existing plasma-based light manipulation schemes (including mirrors [5], gratings [6–8], amplifiers [9,10], and compressors [11]), raising the possibility of an entirely plasma-based

laser system operating at fluences many orders of magnitude larger than conventional laser systems.

This work was performed under the auspices of the U.S. Department of Energy by Lawrence Livermore National Laboratory under Contract No. DE-AC52-07NA27344. This work was supported by the LLNL-LDRD Program under Project No. 42074. We acknowledge the allocation of computational resources under the Grand Challenge program at Lawrence Livermore National laboratory, as well as EPSRC Grant No. EP/K504178/1 and No. EP/L000644/1. Finally, we thank the staff of the Jupiter Laser Facility and Suzanne Ali for enabling a successful experimental campaign.

*turnbull2@llnl.gov

[1] J. Nuckolls, A. Thiessen, L. Wood, and G. Zimmerman, Nature (London) **239**, 139 (1972).
[2] B. A. Remington, D. Arnett, R. P. Drake, and H. Takabe, Science **284**, 1488 (1999).
[3] T. Tajima and J. M. Dawson, Phys. Rev. Lett. **43**, 267 (1979).
[4] W. P. Leemans, B. Nagler, A. J. Gonsalves, C. Toth, K. Nakamura, C. G. R. Geddes, E. Esarey, C. B. Schroeder, and S. M. Hooker, Nat. Phys. **2**, 696 (2006).
[5] C. Thaury, F. Quere, J.-P. Geindre, A. Levy, T. Ceccotti, P. Monot, M. Bougeard, F. Reau, P. d'Oliveira, P. Audebert, R. Marjoribanks, and P. Martin, Nat. Phys. **3**, 424 (2007).
[6] P. Michel, L. Divol, E. A. Williams, S. Weber, C. A. Thomas, D. A. Callahan, S. W. Haan, J. D. Salmonson, S. Dixit, D. E. Hinkel, M. J. Edwards, B. J. MacGowan, J. D. Lindl, S. H. Glenzer, and L. J. Suter, Phys. Rev. Lett. **102**, 025004 (2009).
[7] S. H. Glenzer *et al.*, Science **327**, 1228 (2010).
[8] J. D. Moody *et al.*, Nat. Phys. **8**, 344 (2012).
[9] G. Shvets, N. J. Fisch, A. Pukhov, and J. Meyer-ter-Vehn, Phys. Rev. Lett. **81**, 4879 (1998).
[10] J. Ren, W. Cheng, S. Li, and S. Suckewer, Nat. Phys. **3**, 732 (2007).
[11] V. M. Malkin, G. Shvets, and N. J. Fisch, Phys. Rev. Lett. **82**, 4448 (1999).
[12] P. Michel, L. Divol, D. Turnbull, and J. D. Moody, Phys. Rev. Lett. **113**, 205001 (2014).
[13] A. K. Lal, K. A. Marsh, C. E. Clayton, C. Joshi, C. J. McKinstrie, J. S. Li, and T. W. Johnston, Phys. Rev. Lett. **78**, 670 (1997).
[14] R. Berger, C. Still, E. Williams, and A. Langdon, Phys. Plasmas **5**, 4337 (1998).
[15] J. Fuchs, C. Labaune, S. Depierreux, H. A. Baldis, and A. Michard, Phys. Rev. Lett. **84**, 3089 (2000).
[16] E. Lefebvre, R. L. Berger, A. B. Langdon, B. J. MacGowan, J. E. Rothenberg, and E. A. Williams, Phys. Plasmas **5**, 2701 (1998).
[17] A. Macchi, M. Borghesi, and M. Passoni, Rev. Mod. Phys. **85**, 751 (2013).
[18] A. Henig, S. Steinke, M. Schnürer, T. Sokollik, R. Hörlein, D. Kiefer, D. Jung, J. Schreiber, B. M. Hegelich, X. Q. Yan, J. Meyer-ter-Vehn, T. Tajima, P. V. Nickles, W. Sandner, and D. Habs, Phys. Rev. Lett. **103**, 245003 (2009).